Chemical Physics Impact 6 (2023) 100205

Contents lists available at ScienceDirect

Chemical Physics Impact

journal homepage: www.sciencedirect.com/journal/chemical-physics-impact

The enhancement effect of Nb over $CeSi_2$ catalyst for the low-temperature NH_3-SCR performance

Lipeng Ding, Shaoxiong Zhang, Qinglong Liu, Peng Yang, Yandi Cai, Wei Tan, Wang Song, Fei Gao *, Lin Dong

State Key Laboratory of Pollution Control and Resource Reuse, School of Environment, Jiangsu Key Laboratory of Vehicle Emissions Control, Center of Modern Analysis, Key Laboratory of Mesoscopic Chemistry of MOE, School of Chemistry and Chemical Engineering, Nanjing University, Nanjing 210023, China

ARTICLE INFO

Keywords:
Low-temperature NH3-SCR activity
Ce-Si mixed oxide
Niobium-modifying
Enhanced surface acidity

ABSTRACT

Tuning the acid site on the surface of the catalyst tends towards facilitating the selective reduction of NO_x by NH_3 (NH_3-SCR). In this study, a set of catalysts for the Nb/$CeSi_2$ with different loadings of niobium were synthesized and evaluated in terms of NH_3-SCR over a broad temperature range. The results indicated that a catalyst for 20Nb/$CeSi_2$ exhibited the best low-temperature NH_3-SCR performance while maintaining excellent SO_2/H_2O resistance. These catalysts were also characterized by BET, XRD, Raman, NH_3-TPD, and H_2-TPR to further explore the correlations between catalyst structure and performance after adding niobium. For the Nb/$CeSi_2$ catalysts, the surface structure was blocked by niobium species, resulting in varying degrees of reduction in the specific surface areas. Also, the total acidity decreased with the declines of the specific surface areas while the acidity per unit was enhanced, which facilitates the occurrence of the SCR reaction. Furthermore, *in situ* DRIFTS results indicated that SCR reaction could occur following the Eley-Rideal (E-R) mechanism and Langmuir-Hinshelwood (L-H) mechanism simultaneously over 20Nb/$CeSi_2$ catalyst, which could be attributed to the interaction between niobium and ceria in favor of the activation of inert surface nitrate, considered the primary factor for the improvement of the catalyst performance at low-temperature.

1. Introduction

Nitrogen oxides (NO_x) from industrial production processes and automobile exhaust emissions seriously pollute the atmospheric environment, causing some environmental problems such as the greenhouse effect, acid rain, ozone depletion, and photochemical smog, which are directly harmful to human health [1]. It is widely accepted that the selective catalytic reduction of NO_x with NH_3 (NH_3-SCR) is one of the most efficient techniques for removing nitrogen oxides, and the catalysts are a key component in these techniques [2]. As we all know, the V_2O_5-WO_3(MoO_3)/TiO_2 catalyst has been used widely as a commercial catalyst to remove NO_x from stationary sources, contributing to good sulfur resistance and stability at 300-400 °C [3]. Nevertheless, its use also encountered some problems, such as the relatively narrow operation temperature window, and the conversion of SO_2 to SO_3 in high-temperature, which also limited the use of V_2O_5-WO_3(MoO_3)/TiO_2 for reactions operating at a lower temperature below 300 °C or even lower like non-electric industries [3,4]. Hence, it is of great significance to develop environment-friendly and low-temperature catalysts as alternatives [5].

Among the many catalytic materials, CeO_2 has been widely used in the SCR catalysis field, attributed to its nontoxic and excellent redox properties, while pure ceria showed poor activity due to its weak surface acidity and low resistance to SO_2/H_2O poisoning [6–8]. To overcome these problems, modified ceria-based catalysts have been investigated by doping with different metal elements [9,10]. In previous work, we also synthesized a promising Ce-Si mixed-oxide catalyst by co-precipitation method, which showed great catalytic activity range from 250 to 400 °C and performed excellent resistance to sulfur and water poisoning if the exhaust gas contains 200 ppm SO_2 and 5 vol% H_2O at 250 °C [11]. However, it still needs to catch up on some inadequate, for instance, the insufficient performance below 250 °C, which needs further improvement to meet practical application needs.

Generally, the acidity and redox properties of catalysts were two crucial factors in improving the catalytic activity for an NH_3-SCR reaction, and it had been proven to be an effective method to improve low-

* Corresponding author.
E-mail address: gaofei@nju.edu.cn (F. Gao).

https://doi.org/10.1016/j.chphi.2023.100205
Received 30 January 2023; Received in revised form 18 March 2023; Accepted 5 April 2023
Available online 6 April 2023

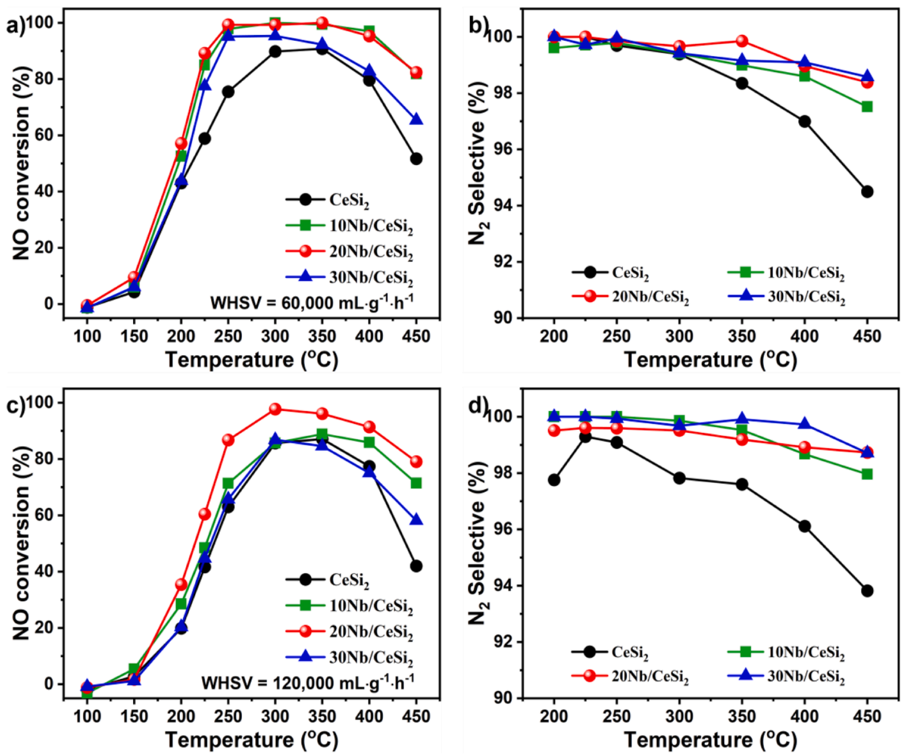

Fig. 1. a) NO conversions and b) N_2 selectivity of related samples as a function of temperature. The feeding gas contains 500 ppm of NH_3, 500 ppm of NO, 4% O_2, Weight hourly space velocity (WHSV) = 60,000 mL·g^{-1}·h^{-1}; c) NO conversions and d) N_2 selectivity of related samples as a function of temperature. The feeding gas contains 500 ppm of NH_3, 500 ppm of NO, 4% O_2, Weight hourly space velocity (WHSV) = 120,000 mL·g^{-1}·h^{-1}.

temperature SCR activity of ceria-based catalysts by adding acidic metallic oxides, such as WO_3, Nb_2O_5, and MoO_3 [12–16]. For example, Liu et al. found that the greater number of acid sites and higher surface concentrations of Ce^{3+} emerging over the surface of CeO_2 with the modification of WO_3, resulting in the 100% NO_x conversion ratio can be reached over WO_3-CeO_2 catalyst by the single step sol-gel from 200 to 450 °C [17]. Li et al. also reported that introducing MoO_3 to CeO_2 can improve the NH_3-SCR activity in a relatively wide temperature range from 200 to 400 °C [18]. Except for the above, the Nb_2O_5-CeO_2 catalyst has also shown great potential for low-temperature activity due to the aid of the acidic nature of NbO_x species in the SCR reaction [19–21]. Qu et al. have reported that the Nb_2O_5-CeO_2 catalyst could achieve over 80% NO conversion in a wide temperature range of 200–450 °C at a GHSV of 120,000 h^{-1} [22]. Although Nb-modified cerium-based catalysts exhibited attractive low-temperature activity, their poor resistance to sulfur poisoning greatly limited their application in practical industrial processes [23]. Therefore, we expected to synthesize a new low-temperature catalyst with superior resistance to SO_2/H_2O poisoning by introducing the niobium to the Ce-Si mixed oxides.

For this work, a wide range of niobium contents was loaded on the Ce-Si mixed oxides catalyst by a common impregnation method. Considering that NH_3-SCR activity is directly related to catalytic surface structure, we first measured the NH_3-SCR activity and N_2-selectivity of all the prepared catalysts. The catalyst exhibiting the best activity was selected for further characterization. Then a series of character technology was carried out systematically and correlated with catalytic activities in the present work.

2. Material and methods

The Ce-Si mixed oxide with a Ce-Si mol ration of 1:2 (denoted as $CeSi_2$) was prepared by a coprecipitation method, as reported previously [11,12]. Firstly, the desired amount of $(NH_4)_2Ce(NO_3)_6$·$6H_2O$ was dissolved into ethanol to obtain a homogenous solution. Then tetraethyl orthosilicate (TEOS) was added dropwise into the solution under continuous magnetic stirring. After stirring for 30 min, aqueous ammonia was added dropwise into the mixed solution until the pH reached 10. The resulting suspension was aged overnight and washed with distilled water. The resulting product was dried at 100 °C for 24 h and calcined at 550 °C for 4 h in the air. For the preparation of the CeO_2, the procedures were just the same as the preparation process of the $CeSi_2$ catalysts yet without the addition of TEOS.

The Nb/$CeSi_2$ catalysts were obtained by impregnating the $CeSi_2$ with $C_4H_4NNbO_9$·nH_2O solution. The controlled amount of Ammonium niobate(V) oxalate hydrate($C_4H_4NNbO_9$·nH_2O) was dissolved into deionized water. Afterward, the $CeSi_2$ powder catalyst prepared previously was put into the solution with continuously stirred for 30 min, then heated in a water bath at 110 °C until all the water evaporated. At last, the resulting solids were dried at 100 °C overnight, followed by calcination at 550 °C for 4 h in the air. The catalysts were denoted as *x* Nb/$CeSi_2$, where *x* represents the mass ratio of Nb_2O_5 to $CeSi_2$. The procedures for the Nb/Ce catalyst were the same as the preparation of the Nb/$CeSi_2$ catalysts.

The NH_3-SCR activity, N_2 selectivity, and NO oxidation were measured in a fixed-bed quartz flow reactor with 100 mg of the prepared catalyst sieved to 40–60 mesh. The reaction conditions were as follows: 500 ppm NO, 500 ppm NH_3 (when used), 200 ppm SO_2 (when used), and 4% O_2 balanced with Ar (when used). The NO, NO_2, NH_3, and N_2O concentrations were measured by an online Thermofisher iS10 FTIR spectrometer equipped with a 2 m path-length gas cell (250 mL volume). In all tests, the total flow rate of the feed gas was controlled at 100 mL/min, which corresponded to a space velocity of approximately 60,000 mL·g^{-1}·h^{-1}. The X_{NO} (NO conversion) and S_{N_2}(N_2 selectivity) were calculated based on the following equations:

$$X_{NO}(\%) = \frac{C_{NO,in} - C_{NO,out}}{C_{NO,in}} \times 100\%$$

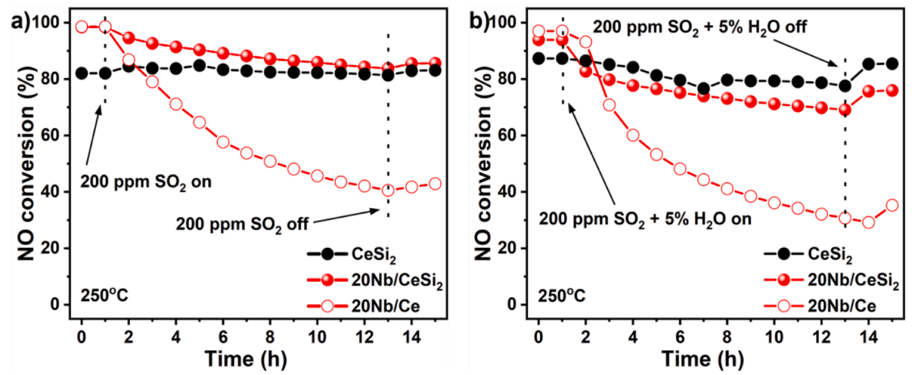

Fig. 2. a) NO conversions of 20Nb/Ce, $CeSi_2$, 20Nb/$CeSi_2$ as a function of reaction time in the presence of 200 ppm SO_2 at 250 °C and b) NO conversions of 20Nb/Ce, $CeSi_2$, 20Nb/$CeSi_2$ as a function of reaction time in the presence of 200 ppm SO_2 + 5 vol% H_2O at 250 °C (The feeding gas contains 500 ppm of NH_3, 500 ppm of NO, 4% O_2, and 200 ppm of SO_2, 5 vol% H_2O (when used), WHSV = 60,000 mL·g^{-1}·h^{-1}.).

$$S_{N_2}(\%) = \frac{C_{NO,in} - C_{NO,out} + C_{NH_3,in} - C_{NH_3,out} - C_{NO_2,out} - 2C_{N_2O,out}}{C_{NO,in} - C_{NO,out} + C_{NH_3,in} - C_{NH_3,out}} \times 100\%$$

Specific surface areas of prepared samples were obtained from N_2 adsorption-desorption isotherms at −196 °C by using a Micromeritics ASAP-2020 analyzer. Before tests, the samples were degassed at 300 °C for 4 h.

X-ray powder diffraction (XRD) patterns were measured on a Philips X'pert Pro-diffractometer with Ni-filtered Cu K_α radiation (0.15408 nm). The range of XRD patterns was 10-80°, and the scan speed was 10°·min^{-1} with a scan step of 0.02°

The transmission electron microscopy (TEM) images were taken on a JEM-2100 instrument operated at 200 kV.

Laser Raman spectra were carried out on a LabRAM Aramis (Japan Horiba) Laser Raman spectrometer with an Ar^+ laser beam with an emission line at 532 nm.

Temperature programmed reduction of hydrogen (H_2-TPR) was performed in a quartz U-tube reactor connected to a thermal conductivity detector (TCD). An H_2-Ar (7% H_2) mixture was used as a reductant. The samples were pretreated with N_2 at 200 °C for 1 h. The measuring temperature range was 100 °C to 800 °C with a ramping rate of 10 °C·min^{-1}.

NH_3-temperature-programmed desorption (NH_3-TPD) was carried out in a fixed-bed quartz flow reactor connected with an online Thermofisher iS10 FT-IR spectrometer equipped with a 2 m path-length gas cell (250 mL volume). Approximately 100 mg of each sample was exposed to the atmosphere with NH_3 at room temperature until adsorption saturated, then Ar was introduced into the quartz tube reactor again to remove the weakly adsorbed NH_3. Afterwards, the samples were heated to 600 °C at a rate of 10 °C·min^{-1} in the flowing Ar (100 mL·min^{-1}).

The *in situ* DRIFT spectra were recorded by a Fourier transform infrared spectrometer (Nicolet Nexus 5700) equipped with an MCT detector cooled by liquid N_2. Before tests, the samples were pre-treated in a N_2 atmosphere at 300 °C for 1 h. The infrared spectra were recorded by collecting 32 scans at a resolution of 4 cm^{-1}.

3. Results and discussion

3.1. NH_3-SCR catalytic performance

For the purpose of investigating the role of niobium species in the catalytic activity of Nb/$CeSi_2$ catalyst, the effect of the catalytic performance and N_2-selectivity of the $CeSi_2$ catalysts with different niobium loading amounts were listed in Fig. 1a. Similar to our previously reported results, the $CeSi_2$ catalyst shown the limited NH_3-SCR performance and its best activity was *ca.* 90% NO conversion at 300 °C [11]. Furthermore, its N_2 selectivity decreased with increasing temperature above 300 °C (Fig. 1b). This phenomenon was attenuated by loading of the NbO_x over a wide temperature range of 250-450 °C, and the selectivity of N_2 was relatively steady. Meanwhile, after loading the catalyst with NbO_x (Nb/$CeSi_2$), the catalyst showed a better performance in the NH_3-SCR than in the $CeSi_2$, with the optimum performance obtained when the loading of NbO_x was 20% and the T_{90} of the 20Nb/$CeSi_2$ catalyst decreased from 300 to 225 °C. Even if in the high WHSV of 12, 0000 mL·g^{-1}·h^{-1} (Fig. 1c and 1d), the 20Nb/$CeSi_2$ catalyst still could maintain the best catalytic performance and more than 80% of NO conversion was achieved in a wide temperature window (250-450 °C). In summary, the 20Nb/$CeSi_2$ is an effective catalyst with high activity at a low temperature. A detailed analysis of the samples was carried out to explain the differences in the catalysis properties, the results of which were presented in the sections.

3.2. Influence of SO_2/H_2O

The sulfur and water resistance of related catalysts at 250 °C was evaluated through long-time resistance tests. The corresponding results were presented in Fig. 2. As depicted in Fig. 2a, with the introduce of 200 ppm SO_2, 20Nb/Ce had a very obvious deactivation, with a rapid decrease in NO conversion from 100% to 40%. It showed that SO_2 caused the rapid deactivation of the niobium species on the surface of CeO_2. Interestingly, thanks to the abundant hydroxyl groups formed on the surface of the $CeSi_2$ catalyst that inhibit the adsorption of sulfur oxides, $CeSi_2$ exhibited an excellent SO_2 resistance comparable to that of 20Nb/Ce [11]. As for the 20Nb/$CeSi_2$ catalyst, the NO conversion initially decreased slightly but remained above 80% during the whole sulfur resistance test, indicating that the 20Nb/$CeSi_2$ catalyst performed superior resistance to sulfur poisoning at lower temperatures than 20Nb/Ce catalysts. Additionally, given that the synergistic effect of water and sulfur dioxide will exacerbate the catalyst deactivation process, the NO conversion of the related catalysts in the coexistence of 5 vol% H_2O and 200 ppm SO_2 was also tested, and the results are shown in Fig. 2b [24,25]. The results were consistent with the above trend of resistance to sulfur, *i.e.*, the Nb-modified $CeSi_2$ catalysts still had the excellent resistance to sulfur dioxide and water vapor. This meant that it was possible to modify $CeSi_2$ catalysts by impregnating them with niobium to improve their performance at low temperatures and retain their excellent resistance to water and sulfur oxides.

3.3. Structural characteristics

As the changes in activity were directly related to structure, the structural properties of the catalysts were further characterized to explore the reasons for the enhancement in activity. XRD was carried out to elucidate the changes in the crystalline state of the catalyst after the

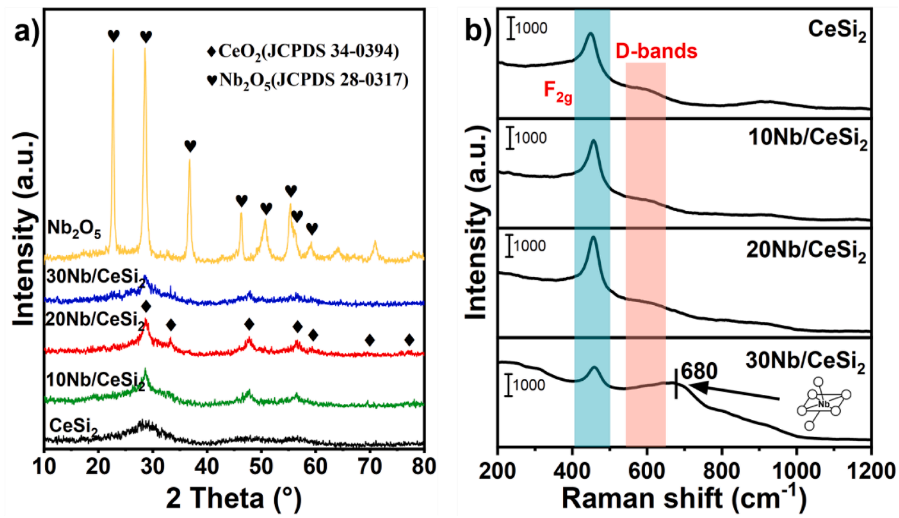

Fig. 3. a) The powder XRD patterns and b) Raman patterns of related samples.

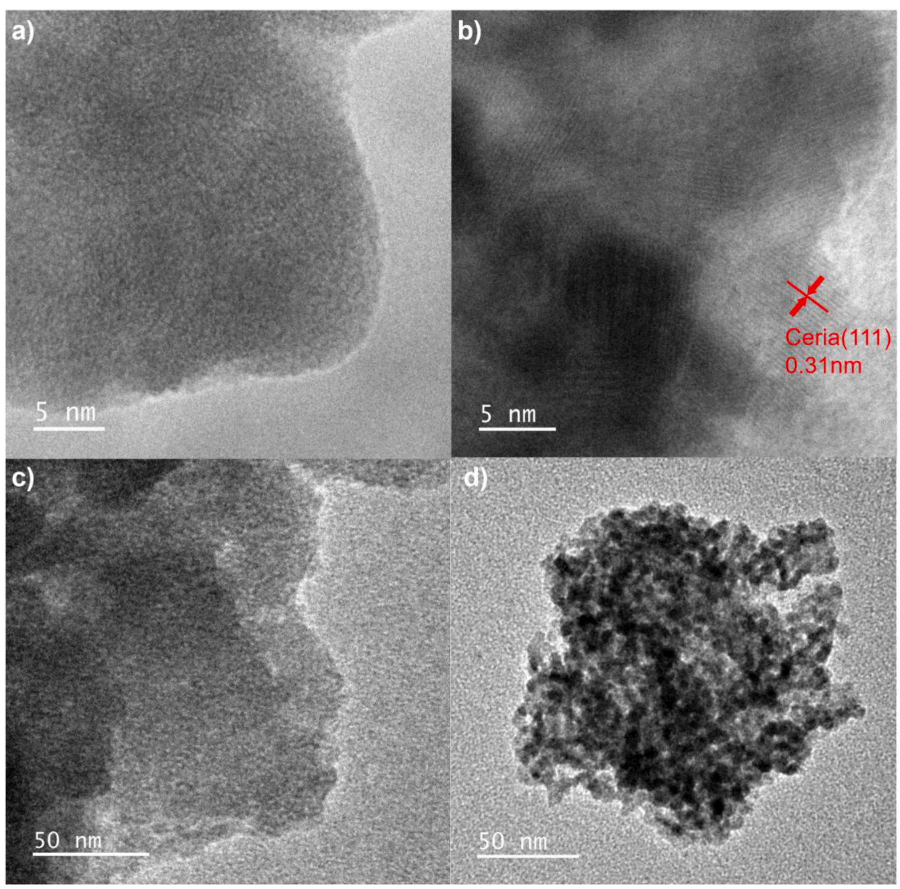

Fig. 4. The HR-TEM images of a) $CeSi_2$ and b) 20Nb/$CeSi_2$ and TEM images of c) $CeSi_2$ and d) 20Nb/$CeSi_2$.

addition of niobium, and the results were displayed in Fig. 3a. Consistent with the description in the literature, the $CeSi_2$ catalyst has no obvious diffraction peaks being detected indicating an amorphous structure was formed [11]. After the loading of niobium species, no typical patterns assigned to Nb_2O_5 crystallites could be observed, which implied that the niobium species are finely dispersed over the $CeSi_2$ in the form of an amorphous state. Nevertheless, with the addition of niobium, the peak appeared at 28°, 33°, 47°, and 56°, which could be indexed to a cubic fluorite-phase CeO_2 structure (JCPDS 34-0394). The appearance of diffraction peaks attributed to CeO_2 proved that the crystallinity of CeO_2 increased [26]. HRTEM was also conducted and the results are presented in Fig. 4. No obvious features could be observed over the $CeSi_2$ catalyst (Fig. 4a). In contrast, the HRTEM image of the 20Nb/$CeSi_2$ catalyst (Fig. 4b) showed distinct lattice fringes related to the CeO_2 (111) crystalline plane with an interplanar spacing of 0.31 nm [14]. Therefore, the results from the HRTEM images illustrated that the introduction of niobium inhibited the interaction between ceria and silicon, resulting in the crystallinity of CeO_2 increased to a certain extent, which was also

Table 1
Textural parameters of the related catalyst samples.

Samples	BET surface area (m^2/g)	Pore volume (cm^3/g)	Pore size (nm)	I_D/I_{F2g} [a]
Nb_2O_5	45	0.178	13.16	/
$CeSi_2$	203	0.165	3.32	0.10
10Nb/$CeSi_2$	136	0.116	3.39	0.06
20Nb/$CeSi_2$	85	0.072	3.40	0.07
30Nb/$CeSi_2$	51	0.045	3.63	/

[a] Calculated by the ratio of the peak area of D-bands and F_{2g} bands of CeO_2.

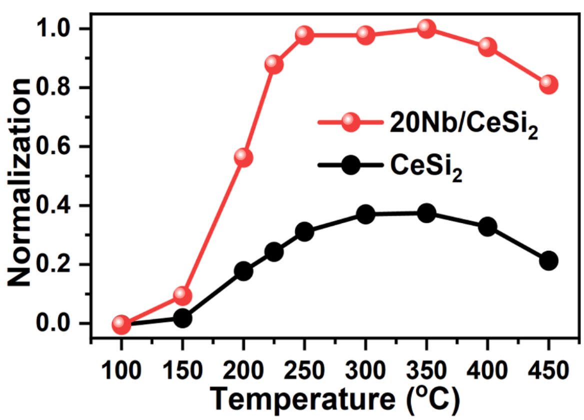

Fig. 5. The specific activity of $CeSi_2$ and 20Nb/$CeSi_2$.

supported by the conclusion of the XRD data [27].

Raman spectra were also collected to explore further the structural properties of the catalysts (Fig. 3b). All the catalysts exhibited a band at *ca.* 460 cm^{-1}, which could be assigned to the F_{2g} vibration mode of the CeO_2 cubic fluorite structure. The intensity of the F_{2g} band on $CeSi_2$ was lower than that on 20Nb/$CeSi_2$, implying the lower crystallinity of $CeSi_2$, which was consistent with the highest specific surface area of $CeSi_2$ [12]. Notably, the band at 680 cm^{-1} associated with surface NbO_x species was observed on 30Nb/$CeSi_2$, suggesting the existence of bulk-like NbO_x species [27]. As reported, pure niobium oxides show poor activity, which could also explain the decrease of catalyst activity when more niobium was added [28–30].

Nitrogen adsorption-desorption experiments were also performed to study the physical properties of the catalysts, the related textural parameters of various catalysts were summarized in Table 1. $CeSi_2$ catalyst had a much larger BET surface area than those loaded with niobium. Adding more niobium would result in a greater loss of the BET surface area of the related catalysts. The reduction in specific surface area should be related to the higher crystallinity of CeO_2 and the plugging of the pore structure by the impregnation of niobium species, which was also supported by the XRD results and the decrease in the pore volume [31,32]. Generally, a high specific surface area benefits the surface adsorption of more reactants and precipitates in the NH_3-SCR reaction. Interestingly, there was an extreme loss on the specific surface area among the catalysts with the increase of niobium loading, which caused little effect on the catalyst activity in this work. Then, the specific activity calculated by further normalizing the specific surface area with the catalyst activity was illustrated in Fig. 5. It can be seen that the specific activity of 20Nb/$CeSi_2$ was about 3 times higher than that of $CeSi_2$ within the reaction temperature window of 200-450 °C. This suggested that the change in structure of the cerium-silica mixed oxide caused by the Nb modification was not the main reason for the variability in the catalytic performance.

3.4. Redox properties

Catalyst structure had a dramatic impact on redox properties, and numerous studies had demonstrated that the redox ability of the catalyst played a crucial role in the SCR reaction, which was also investigated based on related tests [33,34]. According to the results of Raman, the band at *ca.* 600 cm^{-1} was related to oxygen defects (D-bands). The peak area ratio of D-bands to the F_{2g} band (I_D/I_{F2g}) could be used to indicate the relative concentration of oxygen defects, which was used as an indicator of the redox capacity of the catalyst [12]. As listed in Table 1, the I_D/I_{F2g} value was decreased with the addition of niobium, which meant that the number of oxygen defects declined. More oxygen defects could significantly promote redox capacity, facilitating reactant activation [35]. The number of oxygen defects declined also meant the redox properties worsened, illustrating that the addition of niobium species caused a reduction in the redox capacity of the catalyst [36].

In general, the enhancement of low temperature activity was also likely to take place via the "fast SCR" route, which was closely related to the oxidation capacity of the catalyst, especially for the oxidation of NO to NO_2. Therefore, the NO oxidation test was carried out to investigate the NO-oxidation characteristics of the relevant samples (Fig. 6a). For $CeSi_2$, the NO oxidation began at about 200 °C and more NO_2 was generated above 250 °C than the 20Nb/$CeSi_2$ catalyst, which meant the introduction of niobium species declined the NO oxidation capacity. It was worth noting that the low-temperature performance was still enhanced while the NO oxidation property declined, that was to say, other factors affected the low-temperature activity. Fig. 6b showed the H_2-TPR profiles of the related samples. For the profile of $CeSi_2$, the peak α at *ca.* 285 °C and the peak β at *ca.* 542 °C could be assigned to the reduction of surface adsorbed oxygen species and surface Ce^{4+}, respectively [11]. After adding niobium, the reduction peak α moved to the higher temperature and the peak area became smaller, revealing the decrease of redox ability after adding niobium species, which was proven by the result of NO oxidation. It should be noted that a new peak γ at *ca.* 700 °C appeared, and the area of peak β decreased to some extent over the Nb/$CeSi_2$ catalyst. According to the previous reports, the

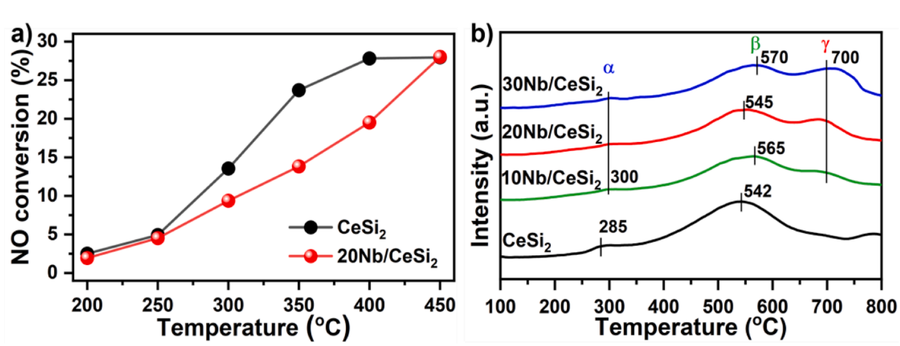

Fig. 6. a) NO oxidation and b) H_2-TPR profiles of related samples.

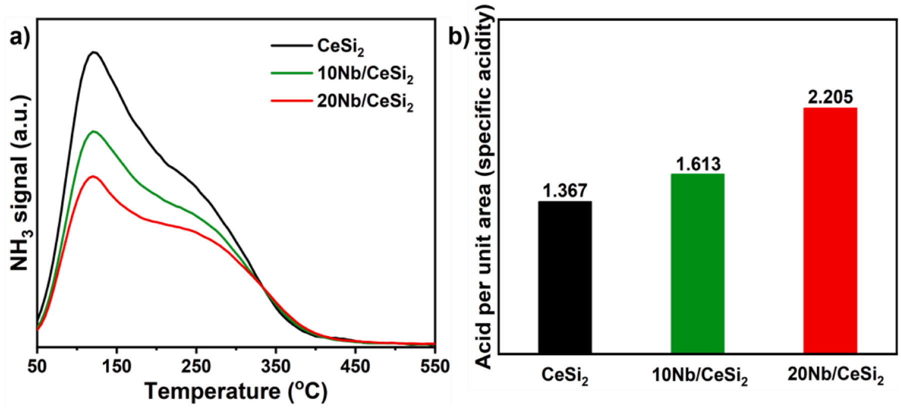

Fig. 7. a) NH_3-TPD profiles and b) acidity normalizing of related samples.

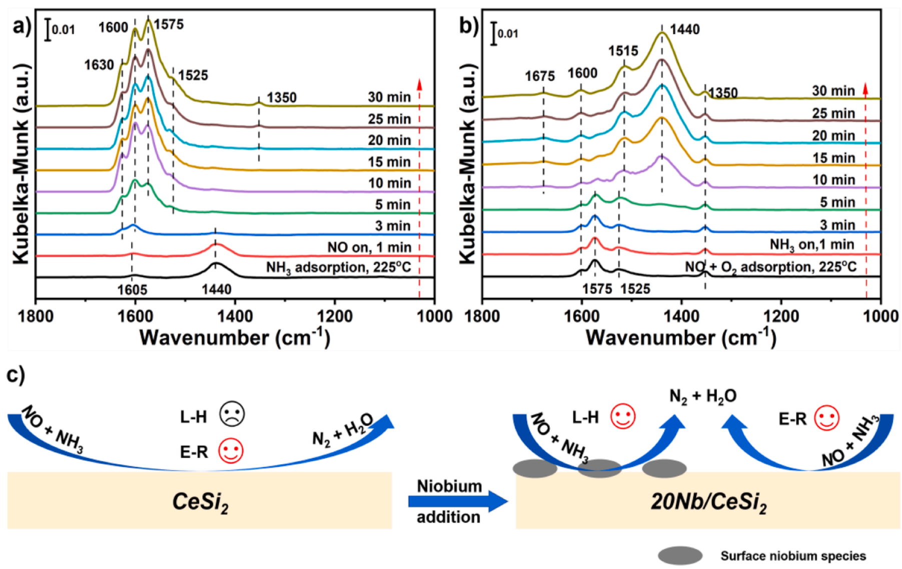

Fig. 8. *In situ* DRIFTS experiments of a) NO + O_2 reacted with pre-adsorbed NH_3 species and b) NH_3 species reacted with pre-adsorbed NO + O_2 over the 20Nb/$CeSi_2$ catalyst at 225 °C and c) the reaction mechanism over $CeSi_2$ and 20Nb/$CeSi_2$.

reduction temperature of niobium oxide was above 800 °C [37]. Hence, the peak γ could be ascribed to the reduction of Ce-O-Nb. In summary, adding niobium species resulted in a reduction in redox capacity, which was unrelated to the factors of activity enhancement.

3.5. Surface acidity

Surface acidity was another important factor influencing the NH_3-SCR performance [37]. Accordingly, the NH_3-TPD profiles of $CeSi_2$ and Nb/$CeSi_2$ were collected to determine the amount of acid sites and acid strength, and the results were shown in Fig. 7a. All the samples exhibited two desorption peaks located in a wide temperature range of 50–450 °C. The first peak at around 150 °C could be assigned to the desorption of weakly surface physically adsorbed ammonia. The other peak at around 250 °C was probably associated with the desorption of chemical adsorbed ammonia on Brønsted and Lewis acid sites [38]. According to the literature, adding niobium normally can improve the catalyst activity by increasing the surface acidity [26]. However, the area of NH_3 desorption peaks over Nb/$CeSi_2$ was smaller than those over the $CeSi_2$ catalyst, illustrating that adding niobium decreased the total amounts of acid sites of the catalysts. Taking in mind the blocking effect of niobium on the pore channel causing the BET surface area to decline, we calculated the acidity per unit area by normalizing the total acidity with the BET surface area (specific acidity). The results were shown in Fig. 7b. It was obvious that the specific acidity enhanced with the addition of niobium, illustrating the catalyst surface acidity could be increased significantly by niobium oxide species due to its acid properties, and the larger specific acidity capacity owing to the introduction of niobium to $CeSi_2$ could be the main reason for its excellent low-temperature activity.

3.6. Reaction mechanism

To further understand the formation and transformation of surface adsorbed species in the NH_3-SCR reaction, *in situ* DRIFTS were recorded as a function of time at 225 °C over the 20Nb/$CeSi_2$ catalyst. To confirm whether the adsorbed NH_3 could react with NO, 20Nb/$CeSi_2$ was exposed to NH_3 for 30 min and followed by purging with N_2 to remove weakly bonded NH_3 species. The result was displayed in Fig. 8a. The bands at 1605 cm^{-1} could be assigned to coordinated NH_3 on Lewis acid sites, and the bands at 1440 cm^{-1} could be attributed to NH_4^+ species on Brønsted acid sites [11,12]. After introduction of NO+O_2, the bands assigned to preabsorbed NH_3 species instantly disappeared, the bands (1350 cm^{-1},1525 cm^{-1},1575 cm^{-1},1600 cm^{-1} and 1630 cm^{-1}) assigned to nitrate species appeared dramatically indicating that the adsorbed NH_3 species over 20Nb/$CeSi_2$ can be reacted directly with NO+O_2 in the gas phase through the Eley-Rideal (E-R) mechanism [11]. The reaction between the NH_3 and pre-adsorbed nitrate species was also conducted. As shown in Fig. 8b, some bands attributed to nitrate species were visible when 20Nb/$CeSi_2$ was exposed to NO+O_2 for 30 min and purged by N_2. The bands center at 1575 cm^{-1} could be attributed to bidentate nitrate, and the bands at 1600 cm^{-1} and 1525 cm^{-1} were assigned to the bridged nitrate and monodentate nitrate, respectively. Upon introducing NH_3 to catalyst pre-adsorbed with NO+O_2, the bands belonging to nitrate species were diminished until dismissed, indicating the surface-adsorbed nitrate species were activated and could participate in the reaction due to the interaction with surface niobium species through the Langmuir−Hinshelwood (L-H) mechanism. That is to say, the NH_3-SCR reaction over Nb/$CeSi_2$ could follow both the L-H and E-R mechanisms, which was different from $CeSi_2$ in that only E-R mechanism was established [11]. Based the results above, the scheme of NH_3-SCR reaction mechanism over $CeSi_2$ and Nb/$CeSi_2$ catalysts was proposed (Fig. 8c).

4. Conclusions

In this work, niobium was used to modify the $CeSi_2$ catalyst to improve the performance of the NH_3-SCR and 20Nb/$CeSi_2$ showed excellent low-temperature activity and better resistance against SO_2/H_2O poisoning. Several characterizations indicated that the enhanced performance of the NH_3-SCR reaction over Nb/$CeSi_2$ catalysts system was due to the combination of both L-H and E-R mechanisms, in which the acidity play the key factor. This work represents a facile and robust strategy for the construction of environment-friendly NH_3-SCR catalysts with satisfied resistance to SO_2/H_2O poisoning.

CRediT authorship contribution statement

Lipeng Ding: Investigation, Visualization, Writing – original draft. **Shaoxiong Zhang:** Validation, Investigation. **Qinglong Liu:** Validation, Formal analysis. **Peng Yang:** Investigation. **Yandi Cai:** Investigation. **Wei Tan:** Conceptualization, Investigation. **Wang Song:** Validation, Methodology. **Fei Gao:** Conceptualization, Writing – review & editing, Funding acquisition, Supervision. **Lin Dong:** Investigation, Resources.

Declaration of Competing Interest

We declare that we do not have any possible conflicts of interests.

Data availability

Data will be made available on request.

Acknowledgements

The financial supports of from the National Natural Science Foundation of China (No. 21972063) and Natural Science Foundation of Jiangsu Province (BK20200012) are gratefully acknowledged.

References

[1] W.B. Chen, R.Q. Zou, X.D. Wang, Toward an Atomic-Level Understanding of the Catalytic Mechanism of Selective Catalytic Reduction of NOx with NH3, ACS Catal. 12 (2022) 14347–14375.
[2] J.Q. E, Z. Shi, Q. Peng, B. Xie, J. Wei, R. Yin, G. Fu, Mechanism, performance and modification methods for NH3-SCR catalysts: a review, Fuel 331 (2023), 125885.
[3] B. Ye, B. Jeong, M.J. Lee, T.H. Kim, S.S. Park, J. Jung, S. Lee, H.D. Kim, Recent trends in vanadium-based SCR catalysts for NOx reduction in industrial applications: stationary sources, Nano Converg. 9 (2022) 51.
[4] Y.W. Wu, X.Y. Zhou, J.L. Zhou, Z. Hu, Q. Cai, Q. Lu, A comprehensive review of the heavy metal issues regarding commercial vanadium-titanium-based SCR catalyst, Sci. Total Environ. 857 (2023), 159712.
[5] Z.H. Lian, Y.J. Li, W.P. Shan, H. He, Recent Progress on Improving Low-Temperature Activity of Vanadia-Based Catalysts for the Selective Catalytic Reduction of NOx with Ammonia, Catalysts 10 (2020) 1421.
[6] L. Han, S. Cai, M. Gao, J.-y. Hasegawa, P. Wang, J. Zhang, L. Shi, D. Zhang, Selective Catalytic Reduction of NOx with NH3 by Using Novel Catalysts: state of the Art and Future Prospects, Chem. Rev. 119 (2019) 10916–10976.
[7] W. Tan, J. Wang, S. Yu, A. Liu, L. Li, K. Guo, Y. Luo, S. Xie, F. Gao, F. Liu, L. Dong, Morphology-Sensitive Sulfation Effect on Ceria Catalysts for NH3-SCR, Top. Catal 63 (2020) 932–943.
[8] R. Xie, L. Ma, K. Sun, G. Zhou, Z. Qu, N. Yan, Catalytic performance and mechanistic evaluation of sulfated CeO(2) cubes for selective catalytic reduction of NO(x) with ammonia, J. Hazard. Mater. 420 (2021), 126545.
[9] M. Cai, X. Bian, F. Xie, W.Y. Wu, P. Cen, Preparation and Performance of Cerium-Based Catalysts for Selective Catalytic Reduction of Nitrogen Oxides: a Critical Review, Catalysts 11 (2021) 361.
[10] C. Tang, H. Zhang, L. Dong, Ceria-based catalysts for low-temperature selective catalytic reduction of NO with NH3, Catal. Sci. Technol. 6 (2016) 1248–1264.
[11] W. Tan, A. Liu, S. Xie, Y. Yan, T.E. Shaw, Y. Pu, K. Guo, L. Li, S. Yu, F. Gao, F. Liu, L. Dong, Ce-Si Mixed Oxide: a High Sulfur Resistant Catalyst in the NH3-SCR Reaction through the Mechanism-Enhanced Process, Environ. Sci. Technol. 55 (2021) 4017–4026.
[12] W. Tan, J. Wang, Y. Cai, L. Li, S. Xie, F. Gao, F. Liu, L. Dong, Molybdenum oxide as an efficient promoter to enhance the NH3-SCR performance of CeO2-SiO2 catalyst for NOx removal, Catal. Today 397 (2022) 475–483.
[13] W. Tan, C. Wang, S. Yu, Y. Li, S. Xie, F. Gao, L. Dong, F. Liu, Revealing the effect of paired redox-acid sites on metal oxide catalysts for efficient NO(x) removal by NH (3)-SCR, J. Hazard. Mater. 416 (2021), 125826.
[14] L.L. Li, C.Y. Ge, J.W. Ji, W. Tan, X. Wang, X.Q. Wei, K. Guo, C.J. Tang, L. Dong, Effects of different methods of introducing Mo on denitration performance and anti-SO2 poisoning performance of CeO2, Chin, J. Catal. 42 (2021) 1488–1499.
[15] Z.B. Xiong, W. Wang, J. Li, L.H. Huang, W. Lu, The synergistic promotional effect of W doping and sulfate modification on the NH3-SCR activity of CeO2 catalyst, Mol. Catal. 522 (2022), 112250.
[16] W.L. Ouyang, Y. Zhou, X.Q. Fei, Y.R. Bai, H.Q. Wang, Z.B. Wu, Simultaneous removal of NO and dichloromethane (CH 2 Cl 2) over Nb-loaded cerium nanotubes catalyst, J. Environ. Sci. 111 (2022) 175–184.
[17] C. Liu, L. Chen, H. Chang, L. Ma, Y. Peng, H. Arandiyan, J. Li, Characterization of CeO2-WO3 catalysts prepared by different methods for selective catalytic reduction of NOx with NH3, Catal. Commun. 40 (2013) 145–148.
[18] X.L. Li, Y.H. Li, Selective Catalytic Reduction of NO with NH3 over Ce-Mo-O-x Catalyst, Catal. Lett. 144 (2014) 165–171.
[19] Z.P. Zhang, Y.Y. Li, P.P. Yang, Y.S. Li, C. Zhao, R.M. Li, Y.J. Zhu, Improved NH_3-SCR $deNO_x$ activity and tolerance to H_2O & SO_2 at low temperature over the $Nb_mCu_{0.1-m}Ce_{0.9}O_x$ catalysts: role of acidity by niobium doping, Fuel 303 (2021), 121239.
[20] N. Ji, J. Yin, Y. Rong, H. Li, Z. Yu, Y. Lei, S. Wang, X. Diao, More than a support: the unique role of Nb2O5 in supported metal catalysts for lignin hydrodeoxygenation, Catal. Sci. Technol. 12 (2022) 3751–3766.
[21] Y.Y. Li, Z.P. Zhang, X.Y. Zhao, Z. Liu, T.R. Zhang, X.Y. Niu, Y.J. Zhu, Effects of Nb-modified CeVO4 to form surface Ce-O-Nb bonds on improving low-temperature NH3-SCR deNO(x) activity and resistance to SO2 & H2O, Fuel 331 (2023), 125799.
[22] R.Y. Qu, X. Gao, K.F. Cen, J.H. Li, Relationship between structure and performance of a novel cerium-niobium binary oxide catalyst for selective catalytic reduction of NO with NH3, Appl. Catal. B Environ. 142 (2013) 290–297.
[23] B. Zhang, L. Deng, M. Liebau, Y. Ren, C. Luo, B. Liu, S. Zhang, R. Glaeser, Promotion effect of niobium on ceria catalyst for selective catalytic reduction of NO with NH3, J. Rare Earths 40 (2022) 1535–1545.
[24] R. Gui, Q. Yan, T. Xue, Y. Gao, Y. Li, T. Zhu, Q. Wang, The promoting/inhibiting effect of water vapor on the selective catalytic reduction of NO(x), J. Hazard. Mater. 439 (2022), 129665.
[25] L. Zhao, Y. Zhang, M.D. Kang, Recent advances in heighten sulfur resistance of SCR catalysts: a review, Environ. Eng. Res. 27 (2022), 200642.
[26] S. Xie, W. Tan, Y. Li, L. Ma, S.N. Ehrlich, J. Deng, P. Xu, F. Gao, L. Dong, F. Liu, Copper Single Atom-Triggered Niobia-Ceria Catalyst for Efficient Low-Temperature Reduction of Nitrogen Oxides, ACS Catal 12 (2022) 2441–2453.
[27] Z. Ma, X. Wu, Z. Si, D. Weng, J. Ma, T. Xu, Impacts of niobia loading on active sites and surface acidity in NbOx/CeO2-ZrO2 NH3-SCR catalysts, Appl. Catal. B Environ. 179 (2015) 380–394.
[28] B. Qin, R.T. Guo, J. Zhou, L.G. Wei, T.Y. Yin, W.G. Pan, Promotional role of Nb modification on $CuCeO_x$ catalyst for low temperature selective catalytic reduction of NO with NH_3: a mechanism investigation, Fuel 329 (2022), 125390.
[29] C. Croise, R. Pointecouteau, J. Akil, A. Demourgues, N. Bion, X. Courtois, F. Can, Insight into the praseodymium effect on the NH3-SCR reaction pathways over W or Nb supported ceria-zirconia based catalysts, Appl. Catal. B Environ. 298 (2021), 120563.
[30] C.-.H. Jeong, H.-.J. Byeon, W.-.J. Jang, K.-.W. Jeon, D.-.W. Jeong, The optimization of Nb loading amount over Cu-Nb-CeO(2)catalysts for hydrogen production via the low-temperature water gas shift reaction, Int. J. Hydrog. Energy 45 (2020) 9648–9657.
[31] L.D. Wang, X.H. Guo, Q.Y. Ye, J.J. Qi, P. Li, F. Yan, Boosting H_2O_2 Activation for the Efficient Degradation of Dimethyl Sulfoxide-Containing Wastewater over Supported Niobia Catalysts, Ind. Eng. Chem. Res. (2022) 14772–14782.
[32] T. Shittu, M. Altarawneh, Investigative properties of CeO2 doped with niobium: a combined characterization and DFT studies, Nanotechnol. Rev. 11 (2022) 191–203.
[33] D. An, Y. Yang, W. Zou, Y. Cai, Q. Tong, J. Sun, L. Dong, Insight into the promotional mechanism of Cu modification towards wide-temperature NH3-SCR performance of NbCe catalyst, Chin. J. Chem. Eng. 50 (2022) 301–309.

[34] J.W. Ji, M.Z. Jing, X.W. Wang, W. Tan, K. Guo, L.L. Li, X. Wang, W. Song, L. J. Cheng, J.F. Sun, W.Y. Song, C.J. Tang, J. Liu, L. Dong, Activating low-temperature NH3-SCR catalyst by breaking the strong interface between acid and redox sites: a case of model $Ce_2(SO4)_3$-CeO_2 study, J. Catal. 399 (2021) 212–223.
[35] S.H. Zhao, Y. Yang, F.K. Bi, Y.F. Chen, M.H. Wu, X.D. Zhang, G. Wang, Oxygen vacancies in the catalyst: efficient degradation of gaseous pollutants, Chem. Eng. J. 454 (2023), 140376.
[36] C.Y. Ge, J.F. Sun, Q. Tong, W.X. Zou, L.L. Li, L. Dong, Synergistic effects of CeO2/Cu2O on CO catalytic oxidation: electronic interaction and oxygen defect, J. Rare Earths 40 (2022) 1211–1218.
[37] W.S. Zhang, X.Y. Shi, Z.D. Yan, Y.L. Shan, Y. Zhu, Y.B. Yu, H. He, Design of High-Performance Iron-Niobium Composite Oxide Catalysts for NH3-SCR: insights into the Interaction between Fe and Nb, ACS Catal 11 (2021) 9825–9836.
[38] X. Wang, Y. Liu, Q. Ying, W. Yao, Z. Wu, The superior performance of Nb-modified Cu-Ce-Ti mixed oxides for the selective catalytic reduction of NO with NH3 at low temperature, Appl. Catal. A Gen. 562 (2018) 19–27.